Available online at www.sciencedirect.com
SCIENCE DIRECT®
Carbohydrate Research 340 (2005) 2154–2162
Carbohydrate RESEARCH

Molecular dynamics investigations of the polysaccharide scleroglucan: first study on the triple helix structure

Antonio Palleschi,[a,*] Gianfranco Bocchinfuso,[a] Tommasina Coviello[b] and Franco Alhaique[b]

[a]*Dipartimento di Scienze e Tecnologie Chimiche, Università di Roma 'Tor Vergata', Via della Ricerca Scientifica, 00133 Roma, Italy*
[b]*Dipartimento di Studi di Chimica e Tecnologia delle Sostanze Biologicamente Attive, Università di Roma 'La Sapienza', P.le Aldo Moro 5, 00185 Roma, Italy*

Received 23 November 2004; received in revised form 10 June 2005; accepted 13 June 2005
Available online 25 July 2005

Abstract—Explicit solvent molecular dynamics (MD) simulations on the triple helix of the polysaccharide Scleroglucan (Sclg) at two temperatures (273 and 300 K) were carried out. Owing to the complexity of the system, a united-atom force field, based on the properly modified GROMACS parameters, was adopted. To test these parameters for our system, MD simulations of the two disaccharidic units, representing the main chain and the side-chain linkages of the Sclg repeating unit, were performed and the results were compared with the literature data. The simulated triple helix of Sclg retained the main experimentally determined features of the polymer. The residence times of the solvent molecules at 273 and 300 K were analyzed. The results show that the more internal water molecules, interacting with the core of the Sclg triplex are not influenced substantially by changing the temperature, on the contrary the water molecules, interacting with the side-chain glucose residues show more significant differences. These data suggest that the more external water molecules, interacting with the side chain, play a major role in the conformational transition experimentally observed at low temperature.

Keywords: Carbohydrate; Scleroglucan; Glucan; Modeling; Gentiobiose; Laminarabiose

1. Introduction

Scleroglucan (Sclg), a polysaccharide secreted by fungi of the genus *Sclerotium*, has a backbone build up by (1→3)-linked β-D-glc*p* units with single glc*p* side chains linked β-(1→6) to every third residue in the main chain (Fig. 1). Sclg exhibits a triple helix conformation (triplex) both in aqueous solution and in the solid state. Solid state (fiber) diffraction reveals a triple helical core sustained by a network of interchain H-bonds among the hydroxyl groups linked to the C-2 atoms of the glucose units of the backbone (O-2(A), O-2(B), and O-2(C) in Fig. 2); the strands are aligned parallel and the side chains are directed away from the helix core.[1,2] Due to its special properties, Sclg has been successfully used for various applications (secondary oil recovery, ceramic glazes, food, paints, cosmetics, etc.).[3] Furthermore, as we have shown in previous papers, the polymer can be used in the formulation of monolithic swellable matrices for modified drug delivery.[4,5] More recently, by addition of borax to a Sclg solution, we have obtained a new hydrogel that, in the form of tablets, is capable of remarkable asymmetric swelling.[6]

Some years ago, we proposed a force field suitable for studying peptides, glycopeptides and carbohydrates making use of energy minimization calculations.[7–9] Using this approach, we have proposed different possible configurations in which three Sclg triplexes arrange to form a channel suitable to contain different drug molecules. We propose that the anomalous swelling of the

* Corresponding author. Tel.: +39 6 72594466; fax: +39 6 72594328; e-mail: antonio.palleschi@uniroma2.it

0008-6215/$ - see front matter © 2005 Elsevier Ltd. All rights reserved.
doi:10.1016/j.carres.2005.06.026

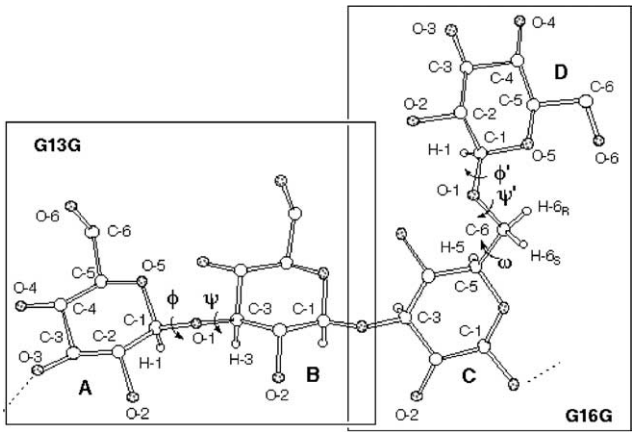

Figure 1. Sclg repeating unit consisting of three β-(13)-D-glucopyranose residues (A–C) with one branched β-(1→6)-D-glucopyranose (D). The torsional angles ϕ and ψ refer to the linear backbone; ϕ', ψ' and ω are the torsional angles relative to the side chain. G13G and G16G correspond to the two disaccharides characterizing the repeating unit, and are known as β-laminarabiose and β-gentiobiose, respectively. For the sake of clarity, only the hydrogen atoms necessary to define the torsional angles are shown. Oxygen atoms are dotted.

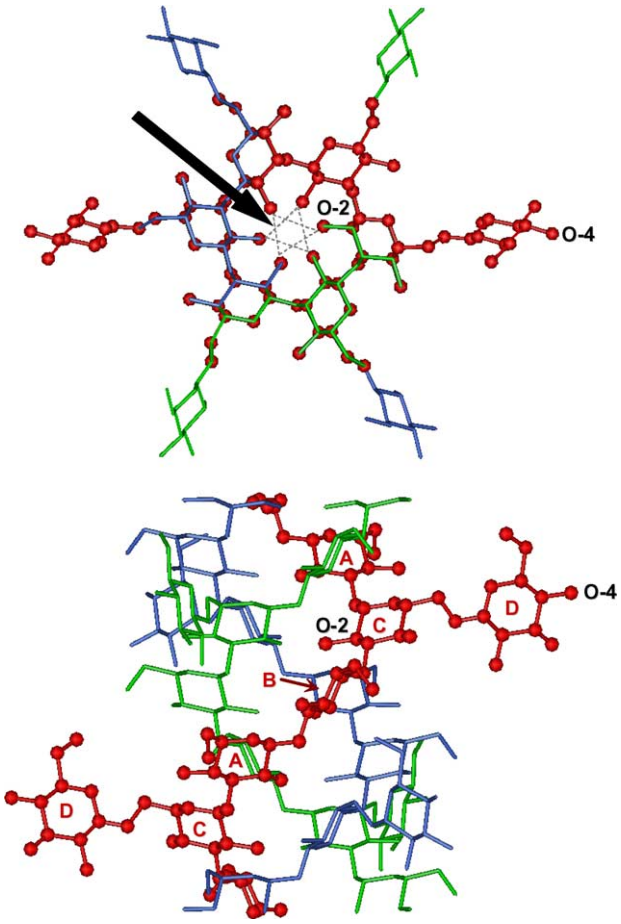

Figure 2. (top) Top view of a fragment of the triple helix of the Sclg. The triple helix is stabilized by inter-chain hydrogen bonds in which each backbone O-2 hydroxyl serves as donor and acceptor to link it to O-2 hydroxyl of a backbone glucose residue in each of the other two chains of the helix. The arrow indicates the network of hydrogen bonds that links the three strands of the triplex. (bottom) Side view of the same triple helix. For the sake of clarity, only one strand is evidenced.

array of Sclg chains, observed when a borax group is added, is due to altered stability of the array structure. In addition, we propose that the release properties for different drug molecules are related to different mobilities through these channels.

Since energy minimization techniques do not provide quantitative data to compare with release experiments, we have undertaken studies with molecular dynamics. Our long-term goal is to perform simulations in which different molecules will be pulled through the channels to simulate drug release.

Because of the very large number of atoms in these system of channels, along with a correspondingly large number of water molecules, we have elected to use a so-called united atoms force field (FFGMX in the GROMACS software package).[10,11] This reduces the required computer time by nearly an order of magnitude.[12] Some modifications have been introduced in the original FFGMX parameters in order to better reproduce the structural features of carbohydrates. Validation of our modifications is emphasized by the reproducibility with previously determined O-6 orientations (*gauche* effect[13–16]) and the *exo*-anomeric effect[17] through studies of the disaccharides laminarabiose,[18–21] β-D-Glc*p*-(1→3)-β-D-Glc*p* (G13G), and gentiobiose,[14,22,23] β-D-Glc*p*-(1→6)-β-D-Glc*p* (G16G), that mimic the glycosidic linkages of the backbone and the side chain, respectively, of the Sclg repeating unit (Fig. 1). We analyzed the behavior of water molecules around the disaccharides and the triplex models, as well as the ω torsional angle transitions in G16G and triplex, both involved in a cooperative transition occurring at about 280 K as underlined by Teramoto and co-workers.[24,25] In addition, the same authors underlined that this transition is strongly depending on the molecular weight.

2. Experimental

2.1. Molecular dynamics settings

According to FFGMX, the CH and CH_2 groups were considered as united atoms, and the hydrogen atoms of the hydroxyl groups were explicitly introduced; the tetrahedral geometry of carbon atoms was maintained by means of improper torsional potentials. The dynamic trajectories were performed using GROMACS software package and analyzed by means of the standard routines of GROMACS and a home-made software. The torsional angles were defined according to IUPAC[26] starting from related angles when the H atoms are lacking. In particular, ϕ, defined as [H-1(A)–C-1(A)–O-1(A)–C-3(B)],

is evaluated as $\phi_o - 120°$, where ϕ_o = [C-2(A)–C-1(A)–O-1(A)–C-3(B)]; ψ, defined as [C-1(A)–O-1(A)–C-3(B)–H-3(B)], is evaluated as $\psi_o + 120°$, where ψ_o = [C-1(A)–O-1(A)–C-3(B)–C-2(B)]; ϕ', defined as [H-1(D)–C-1(D)–O-1(D)–C-6(C)], is evaluated as $\phi'_o + 120°$, where ϕ'_o = [O-5(D)–C-1(D)–O-1(D)–C-6(C)]; and ω, defined as [O-1(D)–C-6(C)–C-5(C)–H-5(C)], is obtained as $\omega_o - 120°$, where ω_o = [O-1(D)–C-6(C)–C-5(C)–O-5(C)] (see Fig. 1).

FFGMX is based on the GROMOS-87 force field, with small modifications not concerning saccharidic molecules. As previously pointed out,[27] these force fields are not able to reproduce inter residue features of saccharidic molecules. To overcome this problem, a new atom type, named OG, was introduced for O-1, with the aim to simulate the different features of these atoms. The OG parameters were obtained from those proposed by Homans,[28] extensively used in the past decade, and based on ab initio calculations at HF/6-31G* level. Summarizing, the changes introduced in FFGMX, were the following: (1) the values of the stretching and bending constants, proposed by Homans, were slightly scaled to be used in FFGMX; (2) the constants used in the energy calculations for the ϕ and ϕ' torsional angles (Richard–Balhemans type) were obtained by fitting those proposed by Homans; (3) only in the case of the (1→6) linkage, the charges of the atoms C-6(C) and O-1(C) were reduced to better mimic the *gauche* effect. Different values for these charges were tested and the best agreement with the NMR experimental data of ω distribution[22] was achieved, when a decrease of about 15% was applied (data not shown). In Table 1, the parameters for the OG atom type, used in our calculation, are reported.

It is well known that the MD simulations should be carried out with explicit inclusion of water molecules,[29] owing to the strong interaction of carbohydrates with water. In the present work, the carbohydrate molecules were solvated in a rectangular box using periodic boundary conditions and SPC/E water model.[30] The box dimensions were $2.8 \times 3.2 \times 2.8$ nm for the G13G unit, $2.6 \times 3.2 \times 2.9$ nm for the G16G unit, and $4.3 \times 4.3 \times 14.4$ nm for the triplex. To obtain a density of about 1 mg/mL, 823, 768, and 7832 water molecules for G13G, G16G, and triplex, respectively, were added. The electrostatic interactions were treated using the PME approach[31] with a cut-off distance equal to 0.9 nm. The temperature was kept constant by coupling, separately for carbohydrate and solvent molecules, to an external bath with coupling constant of 0.1 ps. An isotropic pressure bath was used, to fix the value of 1 atm, with a coupling constant equal to 1 ps.[32] After energy minimization, all systems were equilibrated by means of MD simulations of 100 ps, constraining the atoms of the solute at their positions through a harmonic potential. Simulations of 30 ns for G13G and G16G disaccharides, and of 8 ns for triplex, by using an integration step size of 1 fs, were performed. In order to assess the presence of the hydrogen bond, the standard criteria of GROMACS software package were used.

The starting conformation for the core of the triplex was taken from X-ray structure for curdlan that has the main features of Sclg.[1,2] Glucose residues were

Table 1. Parameters of the OG atom type[a]

Bond	K_{str} (kJ nm^{-2} mol^{-1})	r_o (nm)
Stretching[b]		
OG–CS1/CS2	251,040	0.142
Angle	K_{ben} (kJ rad^{-2} mol^{-1})	θ_0 (°)
Bending[b]		
CS1–OG–CS1	228.800	116.4
CS1–OG–CS2	228.800	116.4
OG–CS1–CS1	265.890	110.1
OG–CS2–CS1	265.890	110.1
OG–CS1–OS	323.136	107.4

Angle	k_0 (kJ mol^{-1})	k_1 (kJ mol^{-1})	k_2 (kJ mol^{-1})	k_3 (kJ mol^{-1})
Dihedral[c]				
OS–CS1–OG–CS1/CS2	5.642	21.945	10.450	−23.408

Angle	k_1 (kJ mol^{-1})	n	χ (°)
Dihedral[d]			
CS1–OG–CS1/CS2–CS1	3.766	3	0

[a] Equivalent atom types are separated by slash. CS1 refers to saccharidic united atom CH1, and CS2 refers to saccharidic united atom CH2.
[b] $E_{str} = 1/2K_{str}(r - r_o)^2$, $E_{ben} = 1/2K_{ben}(\theta - \theta_o)^2$: the K_{str} and K_{ben} (from Ref. 28) were properly rescaled.
[c] $E_{dh} = \Sigma\, k_n(\cos(180 - \phi))^n$ (Richard Balhemans type): the k_n values were obtained by fitting the parameters of the β-glycosidic torsional angles.[28]
[d] $E'_{dh} = k_1(1 + \cos(n\psi - \chi))$: default FFGMX parameters relative to all the *–OS–CS1–* dihedral angles.

added to every third glucose in the triplex model with β-(1→6) linkages having the conformation found in crystalline gentiobiose. Each of the three strands of the triplex had 13 tetrasaccharide repeat units, for a total of 156 glucose residues.

2.2. Analysis of simulation data

To compare the dynamic results with the NMR data, the hetero-nuclear $^3J_{C,H}$ coupling constants (Hz) for G13G were evaluated according to the generalized Karplus equations proposed by Tvaroska et al.[33]:

$$^3J_{\text{C-1(A),H-3(B)}} = 5.7\cos^2\psi - 0.6\cos\psi + 0.5 \quad (1.1)$$

$$^3J_{\text{C-3(B),H-1(A)}} = 5.7\cos^2\phi - 0.6\cos\phi + 0.5 \quad (1.2)$$

In the case of G16G, the comparison with experimental hetero-nuclear $^3J_{C,H}$ coupling constants was carried out using both the relationships reported by Spoormaker et al.[34]

$$^3J_{\text{C-4(C),H-6(C)}S/R} = 3.09 - 0.38\cos(\omega_J - 5.53) + 2.57\cos(2(\omega_J - 5.53)) \quad (2)$$

and the more recent generalized equations derived by Tvaroska et al.[33,35]

$$^3J_{\text{C-4(C),H-6(C)}S/R} = 0.52 + 5.8\cos^2\omega_J - 1.6\cos\omega_J + 0.28\sin 2\omega_J - 0.02\sin\omega_J \quad (3)$$

where ω_J is the dihedral angle involving the atoms C-4(C)–C-5(C)–C-6(C)–H-6(C)$_{R/S}$ that correspond to ω, for the hydrogen in configuration *S*, namely H-6(C)$_S$, and $\omega + 120°$ for the other one in configuration *R*, H-6(C)$_R$ (see Fig. 1). Average values of the homonuclear $^3J_{H,H}$ coupling constants (Hz) between the hydrogen linked to C-5, namely H-5(C), and the two hydrogen atoms linked to C-6 in the configurations *R* and *S*, were calculated using the following equations derived by Stenutz et al.[36]

$$^3J_{\text{H-5(C),H-6(C)}R} = 5.08 + 0.47\cos\omega_O - 0.12\cos 2\omega_O + 0.90\sin\omega_O + 4.86\sin 2\omega_O \quad (4.1)$$

$$^3J_{\text{H-5(C),H-6(C)}S} = 4.92 - 1.29\cos\omega_O + 4.58\cos 2\omega_O + 0.05\sin\omega_O + 0.07\sin 2\omega_O \quad (4.2)$$

where ω_O denotes the angle [O-5(C)–C-5(C)–C-6(C)–O-1(D)].

In order to obtain the residence times of single water molecules around different oxygen atoms, the approach used by Engelsen et al.[37] was employed. The water molecules with the oxygen atom inside a sphere of radius equal to 0.35 nm, centered on a selected saccharidic oxygen atom, were considered. In the case of triplex, all the 39 equivalent oxygen of our model (one for each repeating unit) were taken into account.

3. Results and discussion

3.1. G13G and G16G simulations

Figure 3 shows a three-dimensional representation of the conformational distribution function during the trajectory of the G13G simulation. The maximum of the distribution, centered at $\phi = 50°$ and $\psi = 21°$ has a statistical weight higher than 84%. Two equivalent secondary minima are also present, the first at $\phi = 50°$ and $\psi = -168°$ and the second one at $\phi = -178°$ and $\psi = 21°$. During the trajectory, two transitions from the deepest energy minimum to these alternative minima were detected, after about 6 and 20 ns for ψ and ϕ angles, respectively (see Fig. 4). The results shown in Figure 3 are in good agreement with the in vacuo surface map obtained, for the same system, by French and coworkers. These authors evaluated the energies either by means of a hybrid model, using both quantum mechanics and molecular mechanics calculations on the whole molecule,[20] or by means of quantum mechanics calculations on tetrahydropyran-based analogs.[21] This agreement, between data related to different environments, can be explained assuming that, in this case, the major contributions to the relative stability of the conformers, namely the *exo*-anomeric effect and the different H-bonds stability, are not significantly influenced by the surroundings.

As reported in Table 2, the $^3J_{\text{C-3(B),H-1(A)}}$ and $^3J_{\text{C-1(A),H-3(B)}}$ average values, calculated using the ϕ and ψ angles from MD simulations (Eqs. 1.1 and 1.2), are in good agreement with those experimentally obtained by Cheetham et al.[18] In addition, the time evolution of the inter-residue H-bonds was analyzed, because the crystallographic structures of β-(1→3)-linked carbohydrates indicate that the H-bonds involving the oxygen atoms O-4(B)–O-5(A) are more stable than those involving O-4(B)–O-6(A) and O-2(B)–O-2(A).[23] Figure 4 shows the existence matrix for different intramolecular H-bonds during the simulation of G13G and the time series of the angles ϕ and ψ; obtained data are in very good agreement with the crystallographic results.

The β-(1→6) linkage represents a challenging target for all the predictive methods, and the validation of the parameters is particularly difficult in this case. The stable orientations for the ω angle are indicated as *gauche–gauche* (*gg*), *gauche–trans* (*gt*) or *trans–gauche* (*tg*), where the first letter refers to the orientation of O-6 relative to O-5 and the second to C-4. Several studies evidenced that this angle displays a preference for *gauche* orientations (*gg* and *gt*).[13–16]

Figure 5 shows the value of the ω angle during the simulation of G16G disaccharide as well as the corresponding probability distribution with a *gg:gt:tg* calculated ratios of 39:54:7. According to previous experimental and computational evidence, the *gauche*

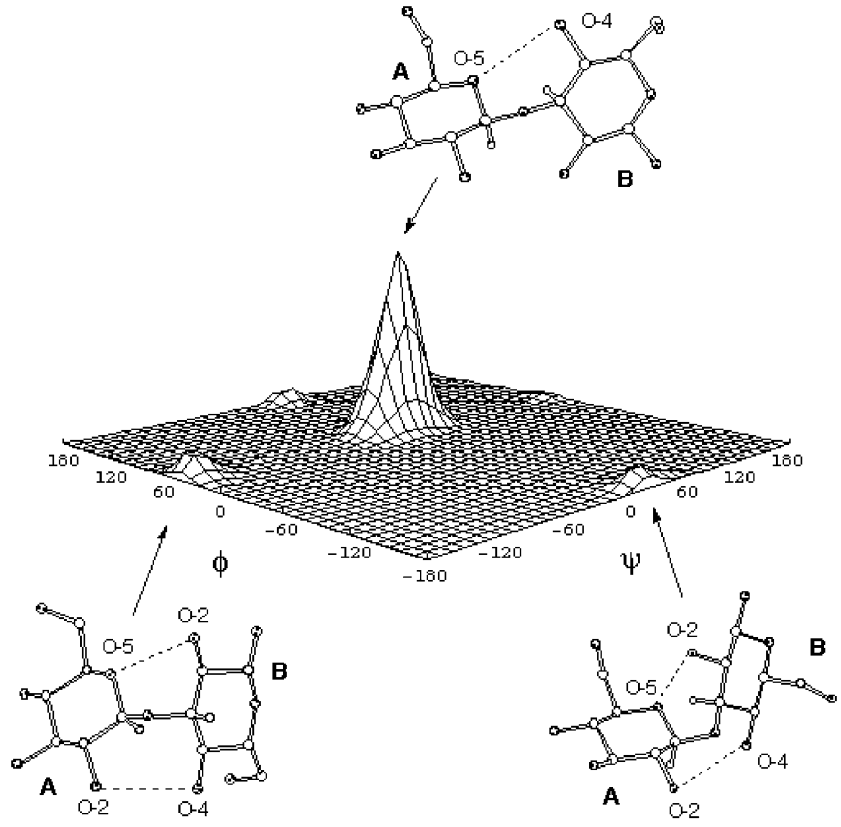

Figure 3. Three-dimensional representation of conformational distribution function for G13G. The conformations corresponding to the minima are also reported. The oxygen atoms involved in the more stable hydrogen bonds are linked by dashed lines.

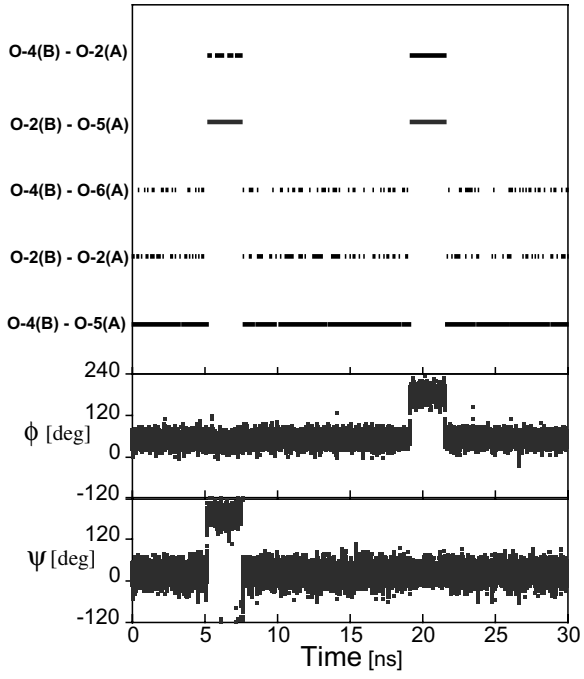

Figure 4. From top to bottom: (a) Existence matrix of the intramolecular H-bonds that appear during the simulation of G13G; (b) trajectory of the glycosidic angle ϕ; (c) trajectory of the glycosidic angle ψ. Note the appearance of the H-bonds between the atoms O-2(B)–O-5(A) and O-4(B)–O-2(A), at about 6 and 20 ns, as a consequence of the ψ and ϕ transitions.

is favored with respect to the trans conformation (*gauche* effect). The relative abundance for *gg* and *gt* is in good agreement with the data obtained by NMR experiments[22] in water–acetone (4:1) (34:66:0). The small discrepancy observed in the case of the *tg* population can be very likely ascribed to the influence of the solvent polarity (water in our simulation, water–acetone in experimental data), because of the high number of saccharidic hydroxyl groups.[29] Furthermore, other NMR data, relative to a G16G derivative in D_2O, showed a *tg* abundance of 3%.[38] In our simulations, the ω average values were 178° (*gg*) and −56° (*gt*), in very good agreement with the data obtained from the two ensembles of β-(1→6)-linked crystallographic structures (175° and −54°)[23] and with the NMR average values[22] as well (172° and −41°). In Table 2, the theoretical coupling constants calculated by Eqs. 2, 3, 4.1 and 4.2, for G16G, are reported. As it can be seen, the simulations allowed reproducing satisfactorily all experimental values.

As shown in Figure 5, the ω angle undergoes many transitions among the *gg*, *gt*, and *tg* states during the simulation. Interestingly, the calculated average time of transition (1 ns) is in very good agreement with the rotational relaxation times of exocyclic side groups of nine different monosaccharides, ranging from 0.5 to 2.1 ns.[39]

Table 2. Experimental and simulated coupling constants for G13G and G16G at 300 K

	$^3J_{C\text{-}1(A),H\text{-}3(B)}$ (Hz)	$^3J_{C\text{-}3(B),H\text{-}1(A)}$ (Hz)	$^3J_{C\text{-}4(C),H\text{-}6(C)S}$ (Hz)	$^3J_{C\text{-}4(C),H\text{-}6(C)R}$ (Hz)	$^3J_{H\text{-}5(C),H\text{-}6(C)R}$ (Hz)	$^3J_{H\text{-}5(C),H\text{-}6(C)S}$ (Hz)
G13G	4.7 ± 0.1[a]	3.9 ± 0.1[a]	—	—	—	—
	4.7 ± 1.1[b]	2.8 ± 1.5[c]	—	—	—	—
G16G	—	—	3.0 ± 0.5[d]	1.0 ± 0.5[d]	6.0 ± 0.1[d]	2.0 ± 0.1[d]
					5.7[f]	2.0[f]
	—	—	3.4 ± 1.1[e]	1.9 ± 1.0[e]		
	—	—	3.9 ± 1.0[g]	1.7 ± 1.0[g]	5.6 ± 1.8[h]	2.6 ± 1.5[i]

[a] Ref. 18.
[b] From Eq. 1.1.
[c] From Eq. 1.2.
[d] Water–acetone (4:1).[22]
[e] From Eq. 2.
[f] Ref. 38.
[g] From Eq. 3.
[h] From Eq. 4.1.
[i] From Eq. 4.2.

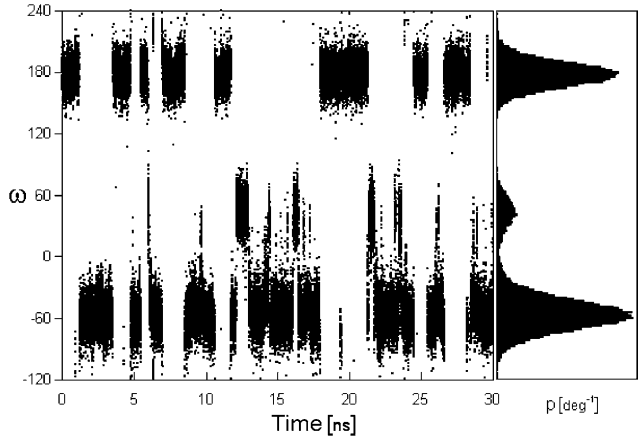

Figure 5. Trajectory of the dihedral angle ω for G16G disaccharide together with its associated probability distribution ($\omega = 180°$ corresponds to *gg*, $\omega = -60°$ to *gt* and $\omega = +60°$ to *tg*).

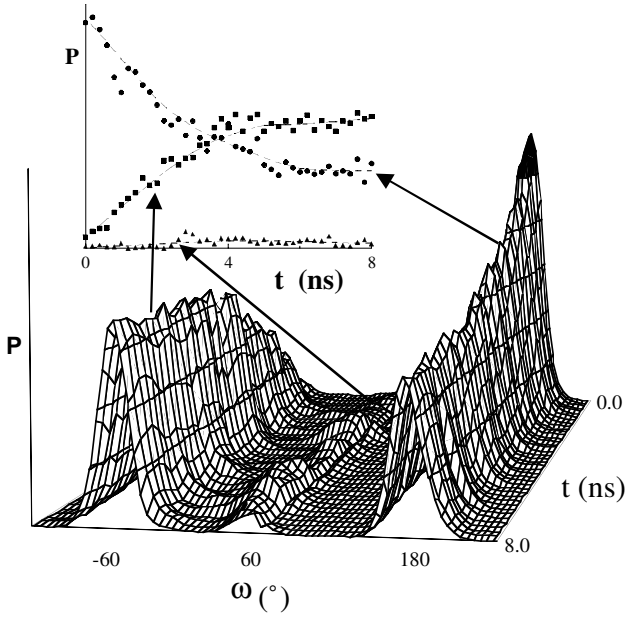

Figure 6. Probability distributions of the dihedral angle ω for the triplex during the simulation, at 300 K. In the inset, the maximum values of the distribution versus time, for three conformations, are reported.

3.2. Scleroglucan simulations

Figure 6 reports the ω probability distribution, at different times, for the triplex at 300 K. The distribution function reaches the same values as those of G16G after about 5 ns. The average time for the ω transitions in triplex increases, with respect to that of G16G, to roughly 2.4 ns that corresponds to about 130 transitions for the 39 side chains during the 8 ns simulation.

The average transition time obtained by analyzing the ω angle distribution for the simulation at 273 K (data not shown) was 4.5 ns. Although, in this case, the time of the simulation (8 ns) was not sufficient to reach the equilibrium, it is important to note the considerable increase of such average transition time. This latter result is in good agreement with the restricted mobility of the ω angle induced by the cooperative conformational transition at about 280 K for the Sclg, as suggested by Teramoto and co-workers.[24,25] Obviously, a quantitative comparison with experimental results is not possible, because this cooperative transition is experimentally strongly dependent on Sclg molecular weight.[24,25]

Figure 7 shows the number of the inter-strand H-bonds involving the hydroxyl groups of the backbone, O-2(A), O-2(B) and O-2(C), normalized by the total number of these atoms in the triplex at 300 K (see Fig. 2). This network of H-bonds is strongly related to the triplex stability, as it can be demonstrated by the disruption of the triple-helical conformation easily achievable by the addition of dimethylsulfoxide (an H-bond breaking compound) to the water solution of

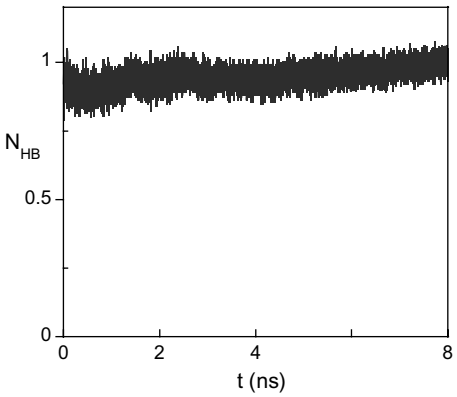

Figure 7. Number of the interstrand H-bonds involving all the O-2 atoms of the backbone (O-2(A), O-2(B), and O-2(C)), normalized by the total number of the same atoms, during the simulation of the triplex at 300 K.

the Sclg.[40] As it can be seen such network of H-bonds is steady during the simulation. This confirms the stability of the triple-helical structure of our model with respect to the stochastic perturbations arising from solvent collisions at 300 K. In addition, it is worth noting that the changes in the ω distribution (side chains) do not affect the inter-strand H-bonds number.

Figure 8 shows a fragment of triplex overlaid each 200 ps, during the last 3 ns of simulation at 300 K (equilibrium for the ω distribution). The backbone triplex retains its conformation and no unwinding process occurs during the simulation. As expected, the side-chain glucose rings show a higher mobility in comparison with the backbone glucose units. Furthermore, it can be pointed out that no remarkable bending of triple helical axis was detected during the simulation, it can thus be confirmed that our model retains the experimental high stiffness of the Sclg triplex.[41]

The residence time distributions around selected oxygen atoms, obtained as described in the experimental section, exhibit an exponential decay, in agreement with Engelsen et al.[37] In particular, the simulations were fitted by the following bi-exponential equation:

$$N_w(t) = x_1 \cdot \exp(-t/\tau_1) + (1 - x_1) \cdot \exp(-t/\tau_2) \quad (5)$$

where $N_w(t)$ is the normalized number of water molecules with residence time t, τ_1 and τ_2 represent the characteristic residence times, and x_1 the fraction of molecules with characteristic residence times τ_1. The fitting parameters, for the last 3 ns of the simulation at 300 K, are reported in Table 3 for all the O-4 atoms. When the same parameters were calculated at different times during the simulation, no remarkable differences were detected (data not shown). Thus, the variation in ω values during the simulation does not affect the water residence features. This is not surprising because the surroundings of each oxygen is slightly influenced by the ω conformation and, as stated above, the average time for

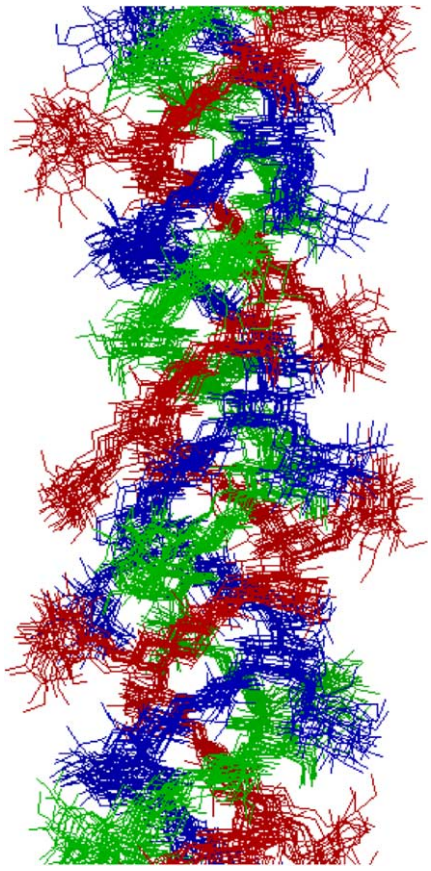

Figure 8. A fragment of triplex overlaid each 200 ps, during the last 3 ns of simulation at 300 K. The overlap is obtained by minimizing the mean square distance among the frames.

Table 3. Characteristic residence times (τ)[a] of the water molecules in the first shell of solvation (300 K)

Oxygen	τ_1 (ps)	τ_1[b] (ps)	τ_2 (ps)	τ_2[b] (ps)
O-4(A)	0.48 ± 0.02[c]	0.58 ± 0.01	2.99 ± 0.15[c]	3.96 ± 0.15
O-4(B)	0.51 ± 0.01[c]	0.55 ± 0.01	3.08 ± 0.15[c]	3.64 ± 0.16
O-4(C)	0.56 ± 0.01[d]	0.57 ± 0.01	3.69 ± 0.14[d]	4.22 ± 0.16
O-4(D)	0.46 ± 0.01[d]	0.54 ± 0.01	2.93 ± 0.11[d]	3.70 ± 0.14

[a] From Eq. 5.
[b] Triplex.
[c] G13G.
[d] G16G.

the ω transitions is two/three orders of magnitude slower than the water residence time. In all cases, τ_1 refers to water molecules (87–92%) residing for about 0.5 ps around the oxygen atoms, and τ_2 values are related to the water molecules with a longer residence time; a remarkable difference between the τ_2 computed in the triplex and the corresponding value of G13G and G16G was observed. Our values for the G13G and G16G are similar to those of Engelsen et al.[37] for similar molecules.

The fitting parameters obtained considering all the water molecules at a distance less than 0.35 nm are

Table 4. Percentage of bonded water molecules, with a residence time more than 20 ps, for six oxygen atoms of the Sclg representative of the core (O-4(A), O-4(B), and O-4(C)) and the side-chain (O-4(D), O-2(D), and O-6(D))

T (K)	O-4(A) (%)	O-4(B) (%)	O-4(C) (%)	O-4(D) (%)	O-2(D) (%)	O-6(D) (%)
273	7.5	7.7	7.8	4.3	4.8	4.2
300	5.1	5.2	5.4	1.9	2.3	2.0

strongly influenced by the large number (more than 87%) of water molecules that interact for only a short time (residence of about 0.5 ps) with a selected oxygen atom. To characterize the water molecules strongly interacting with the solute, in Table 4 the percentages of water molecules with residence time of more than 20 ps at two different temperatures are reported. Two different behaviors of the water are present. In one, the water molecules interact with the oxygen atoms of the triplex backbone (O-4(A), O-4(B), and O-4(C)) with slightly different residence times for the two temperatures (300 and 273 K). In contrast, the water molecules that interact with the oxygen of the side-chain residues (O-2(D), O-4(D), and O-6(D)) have residence times that depend more strongly on the temperature. These data suggest that the more external water molecules, being more influenced by the temperature, are consistently involved in the conformational transition experimentally detected at about 280 K for scleroglucan. On the contrary, the inner water molecules, interacting with the oxygen atoms of the triplex backbone, form a scaffold essentially retained also at higher temperature (300 K) supporting the idea that these molecules are only marginally involved in such transition.[24,25]

4. Conclusions

In order to study the complex structure of the polysaccharide Sclg, we added to FFGMX in the GROMACS software package a new atom type and related parameters, to better take into account *exo-anomeric* and *gauche* effects. These parameters reproduced the main features of laminarabiose and gentiobiose. The simulated Sclg, consisting of 3 strands of 13 tetrasaccharide residues each, retained the properties of the polymeric chain. In particular, the interchain H-bonds between O-2 atoms were mostly retained during the simulation. This confirmed the idea that this H-bond network is responsible for both the stability and stiffness of the triple helix of Sclg and other β-(1→3) glucans. The flexibility of the ω torsional angle, directly involved in the conformational transition at about 280 K for high molecular weight polymer, is strongly temperature dependent, as shown by the transition average times at different temperatures. The analysis of the solvent persistence times at two different temperatures (300 and 273 K) showed that two kinds of water molecules, interacting with the triplex, are present. The first kind, constituted by the water molecules near the Sclg backbone, essentially retains its properties at both the analyzed temperatures. In contrast, the water molecules interacting with oxygen atoms of the side-chain glucose residues are more influenced by the temperature decrease. This suggests that only the second kind of water molecules are directly involved in the reported highly cooperative transition.

Acknowledgements

This work was supported by MIUR. A.P. and G.B. thank Prof. Basilio Pispisa for helpful discussions.

References

1. Norisuye, Y.; Yanaki, T.; Fujita, H. *J. Polym. Sci., Polym. Phys.* **1980**, *18*, 547–558.
2. Bluhm, L. T.; Deslandes, Y.; Marchessault, R. H.; Perez, S.; Rinaudo, M. *Carbohydr. Res.* **1982**, *100*, 117–130.
3. Giavasis, I.; Harvey, L. M.; McNeil, B. Scleroglucan. In *Biopolymers: Polysaccharides II*; De Baet, S., Vandamme, E. J., Steinbuchel, A., Eds.; Wiley-VCH: Weinheim, 2002; Vol. 6, pp 37–60.
4. Coviello, T.; Grassi, M.; Rambone, G.; Santucci, E.; Carafa, M.; Murtas, E. *J. Control. Rel.* **1999**, *60*, 367–378.
5. Coviello, T.; Grassi, M.; Rambone, G.; Alhaique, F. *Biomaterials* **2001**, *22*, 1899–1909.
6. Coviello, T.; Coluzzi, G.; Palleschi, A.; Grassi, M.; Cantucci, E.; Alhaique, F. *Int. J. Biol. Macromol.* **2003**, *32*, 83–92.
7. Palleschi, A.; Crescenzi, V. *Gazz. Chim. It.* **1985**, *115*, 243–245.
8. Chiessi, E.; Palleschi, A.; Paradossi, G.; Venanzi, M.; Pispisa, B. *J. Chem. Res.* **1991**, *9*, 2453–2484.
9. Chiessi, E.; Branca, M.; Palleschi, A.; Pispisa, B. *Inorg. Chem.* **1995**, *34*, 2600–2609.
10. Berendsen, H. J. C.; van der Spoel, D.; van Drumen, R. *Comput. Phys. Commun.* **1995**, *91*, 43–56.
11. Lindhal, E.; Hess, B.; van der Spoel, D. *J. Mol. Mod.* **2001**, *7*, 306–317.
12. Oostembrink, C.; Villa, A.; Mark, A. E.; Van Gusteren, W. F. *J. Comput. Chem.* **2004**, *25*, 1656–1676.
13. Jeffrey, G. A.; McMullan, R. K.; Takagi, S. *Acta Crystallogr. B* **1977**, *33*, 728–737.
14. Marchessault, R. H.; Perez, S. *Biopolymers* **1979**, *18*, 2369–2374.
15. Nishida, Y.; Ohrui, H.; Meguro, H. *Tetrahedron Lett.* **1984**, *25*, 1575–1578.
16. Wolfe, S. *Acc. Chem. Res.* **1972**, *5*, 102–111.
17. Lemieux, R. U.; Koto, S.; Voisin, D. *ACS Symp. Ser.* **1979**, *87*, 17–29.
18. Cheetham, N. W. H.; Dasgupta, P.; Ball, G. E. *Carbohydr. Res.* **2003**, *338*, 955–962.

19. Structures of LAMBIO, QUCXER and WAGBOV from Cambridge Crystallographic Data Centre are available at: http://www.ccdc.cam.uk/prods/csd.html.
20. French, A. D.; Kelterer, A.; Johnson, G. P.; Dowd, M. K.; Cramer, C. J. *J. Mol. Graph. Model.* **2000**, *18*, 95–107.
21. French, A. D.; Kelterer, A.; Johnson, G. P.; Dowd, M. K.; Cramer, C. J. *J. Comp. Chem.* **2001**, *22*, 65–78.
22. Poppe, L. *J. Am. Chem. Soc.* **1993**, *115*, 8421–8426.
23. Kony, D.; Damm, W.; Stoll, S.; Hunemberger, P. H. *J. Phys. Chem. B* **2004**, *108*, 5815–5826.
24. Itou, T.; Teramoto, A.; Matsuo, T.; Suga, H. *Carbohydr. Res.* **1987**, *160*, 243–257.
25. Teramoto, A.; Gu, H.; Miyazaki, Y.; Sorai, M.; Mashimo, S. *Biopolymers* **1995**, *36*, 803–810.
26. IUPAC-IUB Commission on Biochemical Nomenclature *J. Mol. Biol.* **1970**, *52*, 1–17.
27. Spieser, S. A. H.; van Kuik, J. A.; Kroon-Batenburg, L. M. J.; Kroon, J. *Carbohydr. Res.* **1999**, *322*, 264–273.
28. Homans, S. W. *Biochemistry* **1990**, *29*, 9110–9118.
29. Kirschner, K. N.; Woods, R. J. *Proc. Natl. Acad. Sci.* **2001**, *98*, 10541–10545.
30. Berendsen, H. J. C.; Grigera, J. R.; Straatsma, T. P. *J. Phys. Chem.* **1987**, *91*, 6169–6171.
31. Essman, U.; Perela, L.; Berkowitz, M. L.; Darden, T.; Lee, H.; Pedersen, L. G. *J. Chem. Phys.* **1995**, *103*, 8577–8592.
32. Berendsen, H. J. C.; Postma, J. P. M.; Di Nola, A.; Haak, J. R. *J. Chem. Phys.* **1984**, *81*, 3684–3690.
33. Tvaroska, I.; Hricovini, M.; Petrakova, E. *Carbohydr. Res.* **1989**, *189*, 359–362.
34. Spoormaker, T.; De Bie, M. J. A. *Recl. Trav. Chim. Pays-Bas* **1978**, *97*, 85–90.
35. Tvaroska, I.; Gajdos, J. *Carbohydr. Res.* **1995**, *271*, 151–162.
36. Stenutz, R.; Carmichael, I.; Widmalm, G.; Serianni, A. S. *J. Org. Chem.* **2002**, *67*, 949–958.
37. Engelsen, S. A.; Monteiro, C.; Hervè de Penhoat, C.; Perez, S. *Biophys. Chem.* **2001**, *93*, 103–127.
38. Ohrui, H.; Nishida, Y.; Watanabe, M.; Hori, H.; Meguro, H. *Tetrahedron Lett.* **1985**, *26*, 3251–3254.
39. Stenger, J.; Cowman, M.; Eggers, F.; Eyring, E. M.; Kaatze, U.; Petrucci, S. *J. Phys. Chem. B* **2000**, *104*, 4782–4790.
40. Kitamura, S.; Hirano, T.; Takeo, K.; Fukuda, H.; Takahashi, K.; Falch, B. H.; Stokke, B. T. *Biopolymers* **1996**, *39*, 407–416.
41. McIntire, T. M.; Brant, D. A. *J. Am. Chem. Soc.* **1998**, *120*, 6909–6919.